공학석사 학위논문

Anionic Surfactant-mediated Mesoporous Silica Particles for Topical Delivery of Glaucoma Drug to the Eye

음이온 계면활성제 매개 메조포러스 실리카 입자를 이용한 녹내장 약물의 국소 점안 전달

2017 년 8 월

서울대학교 대학원

협동과정 바이오엔지니어링전공

고 송 아

Abstract

Anionic Surfactant-mediated Mesoporous Silica Particles for Topical Delivery of Glaucoma Drug to the Eye

Song Ah Ko
Interdisciplinary Program in Bioengineering,
College of Engineering,
The Graduate School
Seoul National University

An anionic surfactant-mediated mesoporous silica (AMS), a class of amine functionalized mesoporous silica, was prepared *via* the $S^-X^+I^-$ mechanism without additional post modification processes in order to act as a carrier for brimonidine – a glaucoma drug - for the first time. Brimonidine (BRT) was used as a model drug for the topical drug delivery system to the eye to confirm the carrier effect of AMS particles. It was developed to resolve the low drug bioavailability of the glaucoma eye drop formulation caused by a very short drug residence time at the preocular surface due to the

physiological eye clearance system. The amine groups at the AMS particle surface not only enhanced the encapsulation of negatively charged BRT into the AMS inner pore, but also allowed a sustained BRT release. AMS spherical particles (~1μm) with high surface area (544.1 m^2/g) were successfully synthesized and fully characterized. Afterwards, BRT was encapsulated into AMS (BRT-AMS) at a reasonable drug loading amount (41.73 μg/mg). I evaluated the *in vitro* drug release profile of BRT-AMS where there was an initial burst of 59% for the first 20 min, followed by a sustained drug release for 8 h. The cytotoxicity test showed no toxicity to human corneal epithelial cells. To confirm the mucoadhesive property of BRT-AMS particles, *in vitro* and *in vivo* mucoadhesion studies were carried out. Approximately 0.6 mg of the 1 mg mucin was adsorbed by 2 mg of BRT-AMS particles and the zeta potential value of BRT-AMS shifted towards that of mucin. Besides, 25% of the mucoadhesive BRT-AMS particles could reside on a rabbit eye even 4 h after administration. *In vivo* experiments determined efficacy by assessing the change in IOP and drug bioavailability through measuring the BRT concentration in the aqueous humor (AH) of a rabbit eye. The decreasing IOP periods were 12 and 6 h after administrating BRT-AMS and Alphagan P (the commercialized medication), respectively. In addition, the BRT concentrations in AH of Alphagan P and BRT-AMS were detected for 5 and 8 h, respectively, confirming the enhanced bioavailability of BRT-AMS. Thus, it is a suitable carrier for the ocular drug delivery.

Keywords: Glaucoma, Mesoporous silica, Mucoadhesion, Ocular Drug Delivery, Brimonidine

Student Number: 2015-22884

Contents

List of Figures

Ⅰ. Introduction

1.1. Glaucoma and the limitation of its treatment

Glaucoma is an eye disorder to damage the optic nerve, which has been reported to be the second leading cause of irreversible blindness (1, 2). This damage is often related to an abnormal increase in intraocular pressure (IOP) (3) and thus, for early treatment of glaucoma, eye drops of the drug lowering the IOP, such as brimonidine, are often prescribed in current clinical settings (4). However, eye drops are limited in low drug bioavailability (< 5%) due to poor drug retention at the preocular space caused by rapid tear clearance and blinking (5, 6). To resolve this, many systems have been proposed to increase its preocular retention property by employing particles, viscous media, in-situ gels and contact lenses as ophthalmic drug carriers (7-10).

1.2. Mucoadhesive carriers for glaucoma drug

Among them, mucoadhesive particles have drawn a great deal of interest as drug carriers for topical delivery to the eye (7, 11, 12). Mucoadhesive particles in nano- or micro-scale can adhere to the mucous layer at the eye surface to improve their retention at the preocular space. Therefore, when loaded with a glaucoma drug, the particles can stay longer at the preocular space and release drug in a sustained manner, hence enhanced ocular drug bioavailability. For this purpose, drug-loaded particles have been prepared for ocular delivery, using many different types of mucoadhesive materials, such as poly(acrylic acid), sodium carboxymethylcellulose, chitosan, and poly(ethylene glycol) (13). To be mucoadhesive, an anionic surface is considered one of the important characteristics (14). In addition, it would be more advantageous with the functional group on the surface that could form

a chemical bond or a hydrogen bond with carboxyl groups abundant in mucin to promote mucoadhesiveness (15).

1.3. Objective and strategy

In this aspect, therefore, I propose the anionic surfactant-mediated mesoporous silica particles (AMS) as carriers for topical delivery of a glaucoma drug, brimonidine. The AMS were first synthesized by Shunai che *et al.* in 2003, where the use of a co-structure directing agent, (3-aminopropyl)triethoxysilane, allows the amine groups to be formed in the mesoporous silica *via* a single step process, unlike the conventional post-synthetic grafting of aminopropylsilanes (16-21). Thus, the AMS would be mucoadhesive due to a hydrogen bond and a chemical bond between the amine groups in the particles and the carboxyl ones in the mucin. In addition, as the particle size and pore volume of the AMS could be relatively easily modulated, a therapeutic agent could be loaded and released in a controlled manner. Given those, I hypothesize that the AMS loaded with a glaucoma drug can be better retained at the preocular surface and release drug in a sustained manner to enhance ocular drug bioavailability.

In this work, I first assessed the AMS herein with X-ray powder diffraction (XRD), N_2 adsorption-desorption and thermogravimetric (TGA) analyses to confirm their successful fabrication. The morphology was examined *via* scanning electron microscopy (SEM) and transmission electron microscopy (TEM). To our knowledge, this is the first study to demonstrate the AMS as glaucoma drug carriers for topical delivery to the eye. For this, therefore, I loaded brimonidine (BRT), which has already been approved in clinical use for glaucoma treatment (22), in the AMS and evaluated the possibility of AMS as a mucoadhesive carrier. BRT was encapsulated into AMS and *in vitro* drug release profile of BRT-AMS was

evaluated. The mucoadhesive property of BRT-AMS was thoroughly assessed using various methods, including adsorbed mucin measurement, zeta potential shift, and quantitative analysis of remaining particles on the rabbit eye. Finally, *in vivo* efficacy and bioavailability tests of BRT-AMS were performed where BRT-AMS prolonged the period of intraocular pressure decrease, indicating its potential as a carrier for effective glaucoma treatment.

Ⅱ. Materials and Methods

2.1. Materials

Sodium dodecyl sulfate (SDS, assay≥99%), (3-aminopropyl)triethoxysilane (APTES, assay =99%), tetraethyl orthosilicate (TEOS, assay=98%), phosphate-buffered saline tablet (0.01M phosphate buffer, pH 7.4), mucin type Ⅲ (bound sialic acid 0.5-1.5%), Schiff's fuchsin-sulfite reagent (suitable for detection of glycoproteins), periodic acid, and acetic acid were purchased from Sigma (Korea). Brimonidine tartrate (BRT, assay>99.8%), proparacaine hydrochloride (Alcaine; 0.5% ophthalmic solution), ethanol (assay=94.5%), and PVA spears were supplied by Nanjing Yuance Industry & Trade (Nanjing, China), Seoul National University Hospital Biomedical Research Institute (Seoul, Korea), Daejung (Korea) and Medimaru (Korea), respectively. Ketamine hydrochloride (Ketamine), xylazine (Rompun), and acepromazine maleate (Sedaject) were obtained by BK Pharm (Korea). Alphagan P (0.15% ophthalmic solution) was given as a gift from Samil Allergan (Korea).

2.2. Preparation of AMS and BRT-AMS particles

Anionic surfactant-mediated mesoporous silica (AMS) particles were synthesized following the procedure reported by Tatsumi *et al*. (23). Sodium dodecyl sulfate (SDS) 1.8 g was dissolved in 200 ml of deionized water and 76 ml of ethanol under stirring at 60 °C. After adding 5.5 g of (3-aminopropyl)triethoxysilane (APTES) to SDS dispersion, tetraethyl orthosilicate (TEOS) 7.9 g was fed dropwise into the aqueous solution as a silica source. Then, pH of the solution was adjusted to 10.0 to protonate the amino groups of APTES by using HCl and the reaction with stirring

continued for 2.5 h followed by aging at static state, 100 °C for 24 h. Molar ratio of the mixture was kept to APTES:TEOS:SDS:H_2O:EtOH = 0.4:0.6:0.1:180:20. The resulting white solid precipitate formed was filtered and washed with 50% ethanol solution before it was dried at 60 °C.

To load the drug of BRT into AMS, 600 mg of calcinated AMS particles were under vacuum at 100 °C to desorb the water and immersed in 20 ml of BRT solution (30 mg/ml). After 2 days, BRT-AMS particles were prepared by filtering with 0.2 μm PVDF filter paper, washing 3 times with ethanol, and drying at 80 °C.

2.3. Characterization of AMS and BRT-AMS particles

To examine the mesopores inside AMS, High resolution X-ray diffractometer (HR-XRD; SmartLab, Rigaku, Japan) and gas sorption analyzer (Autosorb-iQ 2ST/MP, Quantachrome Instruments, US) were used. XRD peaks of AMS before/after calcination and BRT-AMS were obtained using Cu Kβ radiation at 40 kV 30 mA over a range of $0.5° < 2\theta < 6°$ with scan step size 0.02°.

After nitrogen adsorption and desorption, the nitrogen isotherms of AMS and BRT-AMS were analyzed. The surface area and the pore size distribution were measured by Brunauer-Emmett-Teller (BET) method and Barrett-Joyner-Halenda (BJH) method, respectively.

The thermograms of AMS before/after calcination and BRT-AMS were acquired by performing Thermogravimetric analyzer and differential scanning calorimeter (TGA-DSC; SDT Q600 V20.9 Build 20, TA Instruments, USA) with heating rate of 5 °C/min from room temperature to

700 °C under nitrogen flow rate 50 ml/min.

Samples of AMS and BRT-AMS were prepared by putting a drop of particle suspension in DI water on a small piece of silicon wafer and drying it at room temperature. The pieces of silicon wafer were attached on SEM mount with carbon tape and it was coated with platinum for 30 seconds at 20 mA (Sputter Coater 108auto, Cressington Scientific Instruments, UK) before imaging *via* Field emission scanning electron microscopy (FE-SEM; JSM-7800F Prime, JEOL Ltd, Japan).

The particle suspensions of AMS and BRT-AMS were made with methanol and a drop of the suspension was laid on copper grid and dried at room temperature before imaging through Transmission electron microscopy (TEM; JEM-2010, JEOL Ltd, Japan).

After fully extracting brimonidine from BRT-AMS particles for 2 days with sonification, the drug loading amount of BRT-AMS was measured *via* High performance liquid chromatography (HPLC; Agilent 1260 series, Agilent Technologies, USA) using Poroshell (120 EC-C18, 4.6 × 100 mm, 2.7 μm-pore, Agilent Technologies, USA). The mobile phase of HPLC measurement was the mixture of 20 mM phosphate buffered saline pH 2.5 and acetonitrile (v/v=87:13) with 1 ml/min of flow rate. The injection volume of samples was 20 μl and the measurement of UV absorbance was at 248 nm.

2.4. *In vitro* drug release profile of BRT-AMS

To assess the *in vitro* drug release profile of BRT-AMS, 10 mg of BRT-AMS was placed in 20 ml of 10 mM phosphate buffered saline pH 7.4 and

incubated in Shaking incubator (SI-600R, Jeio Tech, Korea) at 37 °C with 125 rpm. Then, 1 ml was acquired without loss of particles and the same volume of fresh buffer was added at the given time points. The samples containing the cumulative released BRT for scheduled intervals were filtered with syringe filter (pore size 200 nm, Whatman, UK) and measured with HPLC as the same protocol for analyzing the loading amount of BRT.

2.5. *In vitro* mucoadhesion study

To study the interaction between BRT-AMS and mucin, two different types of methods were assessed. First, the amount of adsorbed mucin by particles was measured *via* UV/VIS spectrophotometer (UV-1800 240 V, Shimadzu, Japan) (24, 25). 4 mg of AMS particles and BRT-AMS particles were each mixed with 2 ml of type III mucin solution (1 mg/ml), vortexed, and incubated at 37 °C for scheduled time points (0.5, 1, and 24 h). After certain time interval, the samples were centrifuged at 13500 rpm for 10 min and 1 ml of the supernatant containing free mucin was added by 100 μl periodic acid diluted with acetic acid before incubated for 2 h at 37 °C. Then, 100 μl of Schiff reagent was mixed to the solution at room temperature for 30 min followed by measuring the absorbance at 560 nm. The absorbance of mucin standard solutions (0.1, 0.25, 0.5, and 1 mg/ml) at 560 nm were also measured and a standard curve was obtained to calculate the amount of the free mucin with no adsorption to particles, which was subtracted from total mucin amount given initially to determine the amount of adsorbed mucin by particles. Second, zeta potential change was evaluated by zeta potential analyzer (ELS-2000ZS, Otsuka Electronics, Japan) after incubating 4 mg of particles with 2 ml of mucin solution (0.5 mg/ml) for 30 min (26, 27). To

confirm the chemical interaction between BRT-AMS and mucin, FTIR analysis (FT-IR Spectrometer; Vertex 70, Bruker, US) was performed.

2.6. Cell cytotoxicity test

The cytotoxicity of BRT-AMS was assessed on human primary corneal epithelial cells (HCECs; PCS-700-010, ATCC, USA) using EZ-Cytox cell viability assay kit (water-soluble tetrazolium salt, WST method). HCECs were cultured in corneal epithelial cell basal medium (PCS-700-030, ATCC, USA) with corneal epithelial cell growth kit (PCS-700-040, ATCC, USA) and maintained at 37 °C in a humidified 5% CO_2. To test the cell cytotoxicity, 500 µl of HCECs suspension (1.0 x 10^5 cells/ml) were seeded on a 24-well plate 24 h before adding BRT-AMS at various concentrations 0.02, 0.05, 0.1, 0.2, 0.5, and 1 mg/ml). After the addition of BRT-AMS to the cells, the plate was incubated at 37 °C for 24 h in a 5% CO_2 humidified atmosphere. Then, 50 µl of WST reagent solution was added to each well and the plate was incubated at 37 °C for an hour to measure the absorbance at 450 and 600 nm by using a microplate reader (SpectraMax 190 Microplate Reader; Molecular devices, New Delhi, Sunnyvale, USA). The cell viability was calculated by the equation: cell viability (%) = [(absorbance at 450 nm of BRT-AMS - absorbance at 600 nm of BRT-AMS) / [(absorbance at 450 nm of untreated control - absorbance at 600 nm of untreated control) x 100] (28).

2.7. Animal experiments

To examine the mucoadhesive property of BRT-AMS, the *in vivo* evaluation on the amount of remaining particles at the eye surface was performed with

healthy and male New Zealand White rabbits (2.5–3.5 kg, Orient Bio Inc., Korea). It was under the approval of the Institutional Animal Care and Use Committee (IACUC No. 13-0101) at the Biomedical Research Institute of the Seoul National University Hospital. The experiment protocols were as same as the previous study by Park *et al.* that the 35 μl of BRT-AMS suspension (52.5 μg BRT/1.26 mg AMS suspended in 35 μl PBS) with 10 mM PBS pH 7.4 was administrated on the lower cul de-sac of the rabbit eye and the eye was wiped with a PVA surgical sponge at the scheduled intervals (0.5, 1, 2, 4, and 12 h after administration) (29, 30). 35 μl of a 0.5% proparacaine eye drop was administrated to locally anesthetize the rabbit's eye before obtaining the remaining particles in the eye. The PVA surgical sponges stained with remaining particles were treated by acid solutions ($HF:HNO_3:H_2O$ = 2:3:4) and microwave digestion to quantify the weight of Si which is main component of AMS by using inductively coupled plasma mass spectrometer (ICP-MS; Agilent 7800, US).

The evaluation of *in vivo* efficacy and drug bioavailability was conducted through measuring the change in intraocular pressure (IOP) and assessing the drug concentration in the aqueous humor (AH), respectively. In this study, Alphagan P, the approved eye drop of bimonidine which lowers IOP, was used as a comparison. To examine *in vivo* efficacy, normal IOP of rabbit eye was measured with a tonometer (Tono-Pen AVIA, Reichert, NY, USA) to get reference values on each rabbit after locally anesthetizing the eye with 35 μl of a 0.5% proparacaine eye drop. And then, 35 μl of Alphagan P 0.15% and 35 ul BRT-AMS suspension containing an equivalent to 52.5 μg of BRT were administrated on the lower cul de-sac of the rabbit eye. In both of them, IOP was measured at the scheduled time points after locally anesthetizing the eye with 35 μl of a 0.5% proparacaine eye drop (29, 31).

I also studied the actual drug content delivered into the eye from the administrated samples such as Alphagan P and BRT-AMS. The rabbits were anesthetized with subcutaneous injection of a concoction of 17.5 mg/kg ketamine, 5 mg/kg xylazine, and 0.2 mg/kg acepromazine about 20 min before obtaining approximately 100 μl of aqueous humor using insulin syringes at scheduled time points. After obtaining the liquid, the rabbits were applied with terramycin, ophthalmic ointment, to prevent infections. The concentration of drug on the samples were measured *via* high performance liquid chromatography (HPLC; Agilent 1260 series, Agilent Technologies, USA) using poroshell (120 EC-C18, 4.6 × 100 mm, 2.7 μm-pore, Agilent Technologies, USA). The mobile phase of HPLC measurement was the mixture of 20 mM phosphate buffered saline pH 2.5 and acetonitrile (v/v=95:5) with 1 ml/min of flow rate. The injection volume of samples was 100 μl and the measurement of UV absorbance was at 248 nm (29).

2.8. Statistical analysis

In the study of change profiles in IOP, drug concentration profiles in AH, and mucin amount adsorbed by particles, statistical significance of the differences between particles such as AMS or BRT-AMS and controls at each time was tested by a paired t-test at a level of $p < 0.05$.

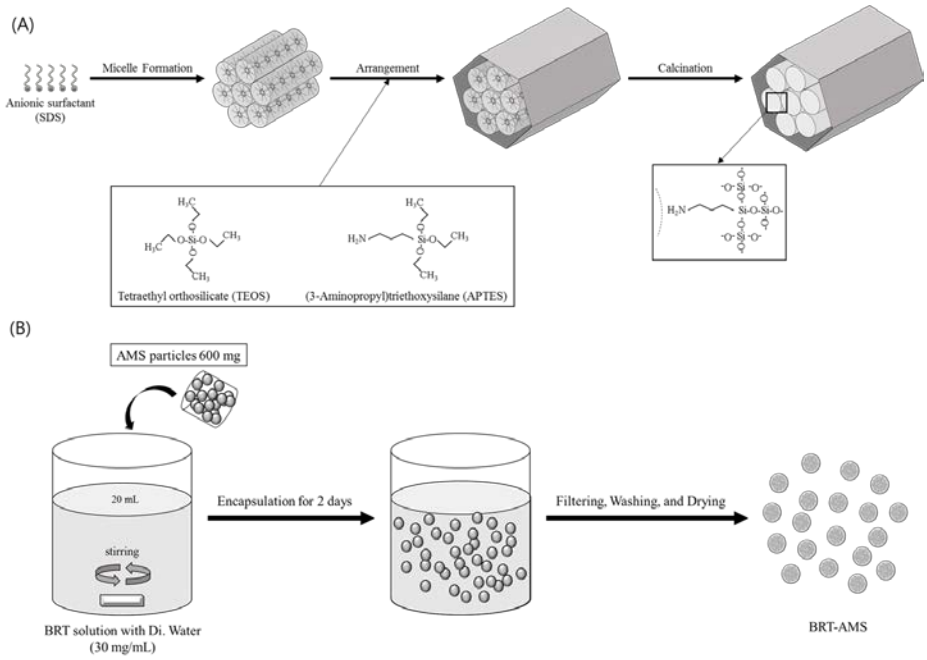

Figure 1. Schematic procedure for (A) synthesizing anionic surfactant-mediated mesoporous silica (AMS) and (B) encapsulating the drug into AMS to prepare BRT-AMS.

Ⅲ. Results

3.1. Characterization of AMS and BRT-AMS particles

The spherical shapes of AMS and BRT-AMS particles were observed to be approximately 1 μm in diameter, as shown in the SEM images (Figure 2). It seemed that the shapes and sizes of the AMS particles were not affected by the presence of the drug in mesopores inside the particles as well as the drug encapsulation process for 2 days in aqueous phase. To minimize irritation to the eye, the particles were synthesized to be less than 10 μm (32).

The as-synthesized AMS had a single broad peak in the range 2θ = 0.5-1° of the XRD pattern like other AMS particles synthesized by the Tatsumi group (23) (Figure 3), indicating disordered mesopores inside AMS particles. The XRD patterns of calcinated AMS and BRT-AMS were similar to that of as-synthesized AMS, which suggested that its mesostructure was well maintained during the calcination and drug encapsulation process.

The thermograms of as-synthesized AMS, calcinated AMS, and BRT-AMS were obtained by TGA (Figure 4). For the first step in temperatures lower than 120 ℃ range, washing solvents (i.e. water and ethanol) trapped inside particles were evaporated. And then, the surfactant was removed from 160 to 380 ℃ in accordance with the previous report by Ramimoghadam *et al*. (33). The decomposition of aminopropyl moieties and the dehydration of surface hydroxyl groups occurred over 250 ℃ as reported by Wiesner *et al*. (34). Thereby, the calcination was performed to remove the surfactant at 400 ℃ for 8h. A few changes were observed in the thermograms of calcinated AMS and BRT-AMS from room temperature to 700 ℃ due to the removal of residual parts such as aminopropyl moieties and moisture at the particle surface. Thus, the encapsulated drug was not the

only factor of the mass loss in the thermograms so that it was not precisely observed as 4.2%.

The BET surface area of AMS was 544.1 m^2/g by using the nitrogen adsorption and desorption method. It was corresponded to other results by Tatsumi *et al.* (23) and AMS particles showed 12 times larger specific surface area than PLGA/PEG nanostructured microparticles (44.2 m^2/g) prepared by Park *et al.* (29). This was attributed to the superior porosity of AMS particles considering that the size of AMS particles was not significantly different from that of the nanostructured PLGA/PEG microparticles (~1.7 μm). The isotherm exhibited a type IV pattern with the typical hysteresis loop (Figure 5) due to the capillary condensation, which is a sign of porosity (35-37). The average pore diameter was 3.8 nm using BJH method and total pore volume was 0.36 cm^3/g, which featured the successful synthesis of AMS (Figure 6).

As shown in the TEM images (Figure 7 (A-B)), calcinated AMS exhibited a wormhole-like structure similar to earlier reports (23, 36) where mesopores inside particles were observed. The calcinated AMS particles were immersed in BRT solution for 2 days at static state to prepare BRT-AMS particles. The drug loading amount of BRT-AMS was 41.73 μg/mg when measuring *via* HPLC after fully extracting the encapsulated drug. As the mesopores inside AMS were filled with BRT, the mesoporosity of BRT-AMS seemed to decrease as shown in TEM images (Figure 7 (C-D)). Moreover, the BET surface area of BRT-AMS was reduced from 544.1 m^2/g to 363.3 m^2/g (Figure 5) due to the encapsulation of BRT into the particles.

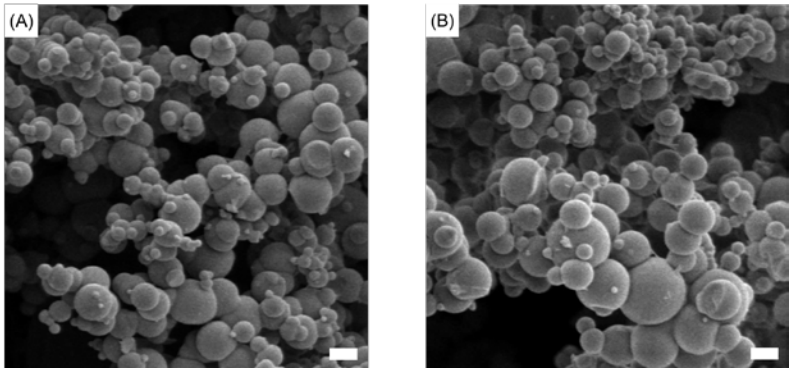

Figure 2. SEM images of (A) AMS and (B) BRT-AMS. The scale bars are 1 μm.

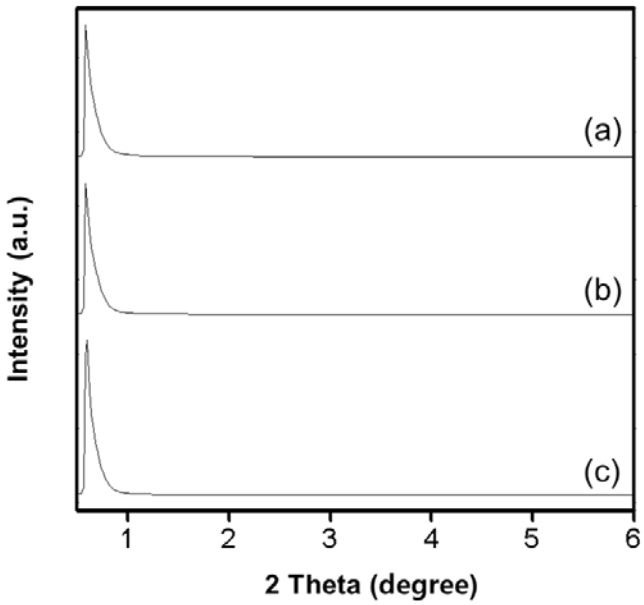

Figure 3. X-ray diffraction (XRD) patterns of (a) AMS before calcination, (b) AMS after calcination, and (c) BRT-AMS.

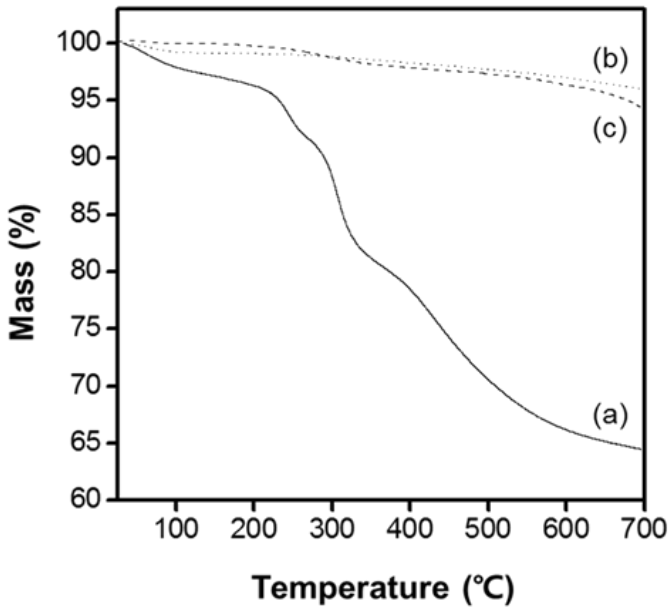

Figure 4. Thermogravimetric analysis (TGA) of (a) AMS before calcination, (b) AMS after calcination, and (c) BRT-AMS.

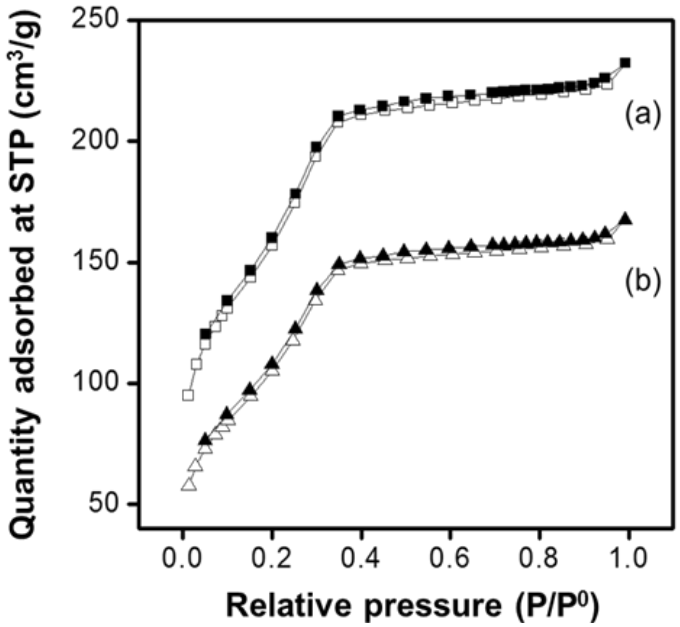

Figure 5. N_2 adsorption-desorption isotherms of (a) AMS and (b) BRT-AMS.

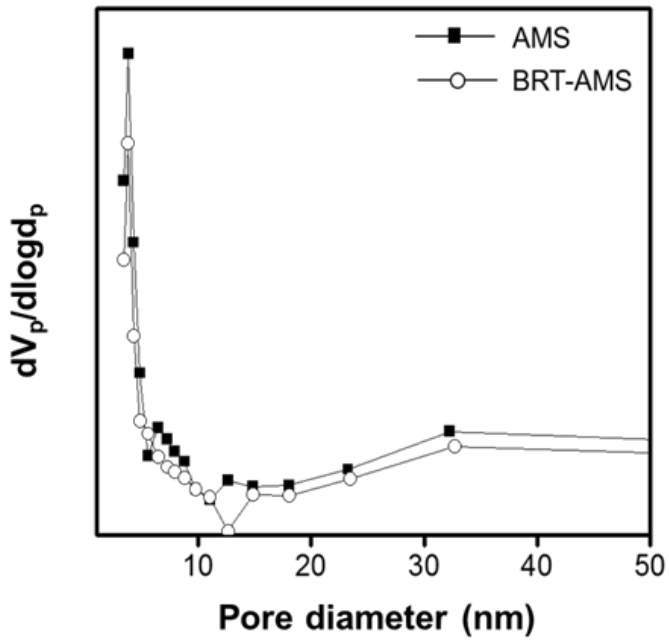

Figure 6. Pore size distribution of AMS and BRT-AMS.

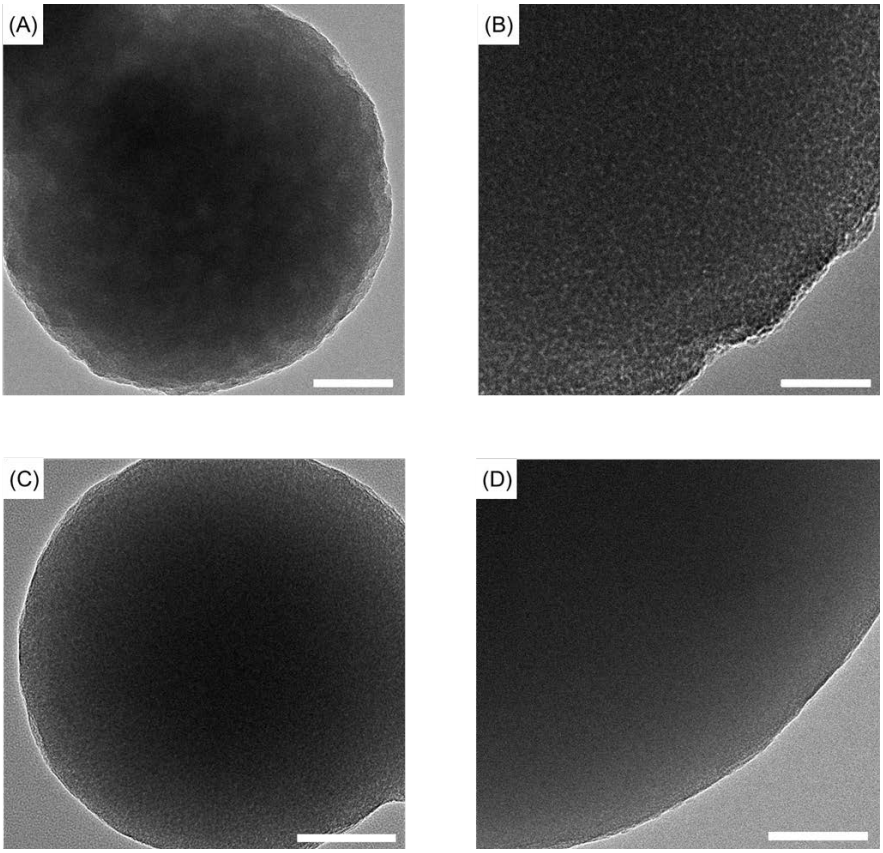

Figure 7. Transmission Electron Microscopy (TEM) images of (A-B) AMS and (C-D) BRT-AMS. The scale bars are 100 nm.

3.2. *In vitro* drug release profile

An *in vitro* drug release study was performed in 10 mM PBS pH 7.4 media with BRT-AMS particles according to the protocol mentioned above. The samples were cautiously obtained on the top of the solution at scheduled time points not to disturb the sunk particles at the bottom of the vials. As shown in Figure 8, a burst release of 59% for the first 20 min was observed due to high solubility in water of BRT (29.85 mg/ml) (38). After that, 90% of the total BRT loading amount was released for 2 h and the sustained release progressed to reach 100% after 8 h. This result indicated that BRT-AMS particles were suitable carriers to the eye because the loaded drug was almost completely released during their residence time on rabbit eye.

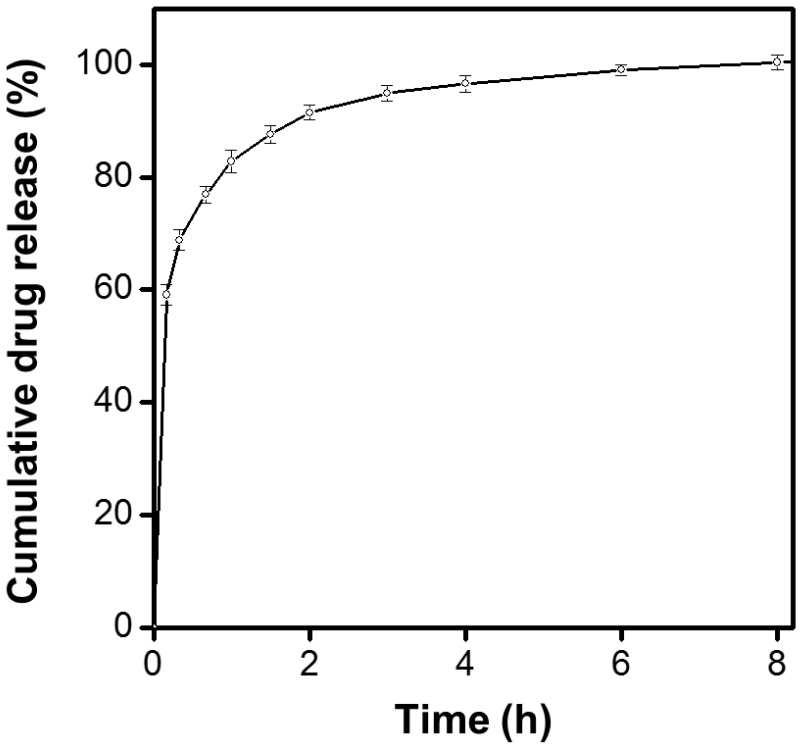

Figure 8. *In vitro* brimonidine release profile of BRT-AMS. Error bars represent standard deviation.

3.3. *In vitro* mucoadhesion study

The amount of mucin adsorbed by the particles was quantitatively analyzed *via* a colorimetric method to assess the mucoadhesive property of BRT-AMS. Both AMS and BRT-AMS showed an increasing trend in the amount of adsorbed mucin over time and had statistical significance when compared at each time point (Figure 9). For 1 mg of mucin, 0.52, 0.55, and 0.59 mg of mucin and 0.61, 0.64, and 0.68 mg of mucin were adsorbed by AMS and BRT-AMS, respectively, at 0.5, 1, and 24 h after mixing mucin and particles. This showed that AMS had good mucoadhesive capability similar to well-known mucoadhesive chitosan microparticles (24, 25). Besides, the zeta potential of BRT-AMS (-63.50 mV) in KCl shifted towards that of the mucin solution (-27.56 mV) after incubation in BRT-AMS with mucin for 30 min, resulting in -43.61 mV (Figure 10) as explained by mucin stuck to the BRT-AMS particle surface.

To further verify the interaction between BRT-AMS particles and mucin, newly formed chemical bonds were confirmed. From the knowledge that mucin has carboxyl groups on sialic acids, amide groups were hypothesized to form when amine-functionalized AMS was administrated to the eye with a mucin layer. The newly formed amide groups between amine groups of AMS and carboxyl groups of mucin were confirmed *via* Fourier transform infrared spectrometer. The amide characteristic peak never found in FTIR spectra of BRT-AMS and mucin (data was not shown) was exhibited near 1275 cm^{-1} (Figure 11) after mixing BRT-AMS particles with mucin solution for 30 min (39). In addition, many peaks of -OH, -NH stretching, -NH bending, Si-O-Si asymmetric stretching, -Si-OH stretching, Si-O-Si symmetric stretching were observed at 3436 and 1636, 2959-2969, 2349, 1086, 946, and 805 cm^{-1}, which indicated that BRT-AMS was well prepared

as other amine-functionalized mesoporous silica materials were (40, 41).

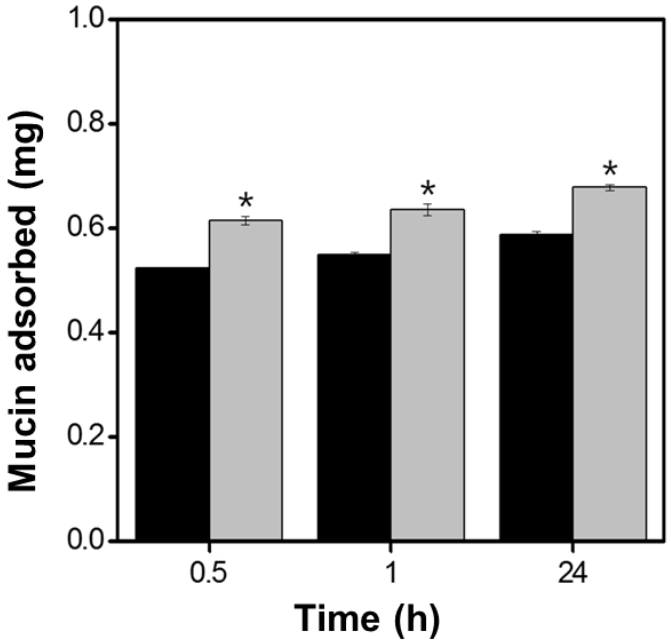

Figure 9. Adsorption kinetics of mucin type Ⅲ with AMS (black) and BRT-AMS (grey). *BRT-AMS was statistically significantly different from AMS ($p < 0.05$). Error bars represent standard deviation.

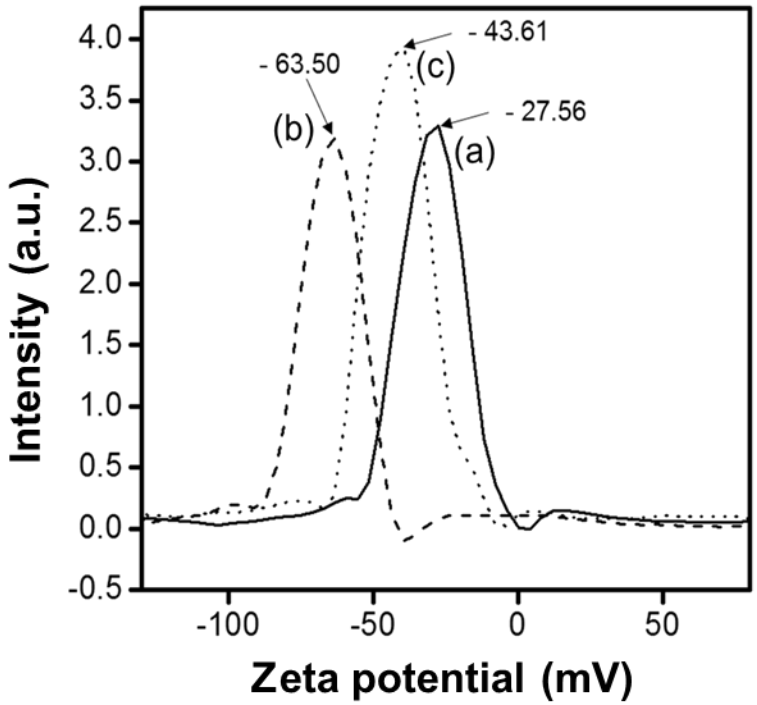

Figure 10. Zeta potential measurement of (a) mucin, (b) BRT-AMS, and (c) BRT-AMS incubated with mucin.

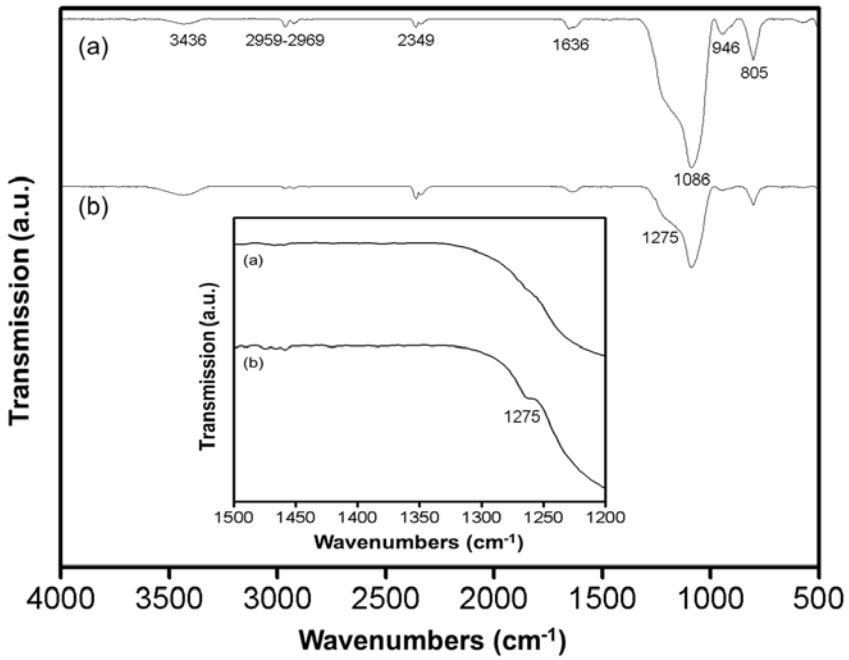

Figure 11. FTIR spectra of (a) BRT-AMS and (b) BRT-AMS with mucin.

3.4. Cell cytotoxicity evaluation

As shown in Figure 12, the BRT-AMS had no toxicity for HCECs up to 1 mg/ml of BRT-AMS suspension when investigating the cell viability by the WST method described above. This result suggests that BRT-AMS particles are biocompatible and are promising ocular drug delivery carriers. The size of the human eye is similar to that of a 6-well plate (10 cm^2) where 2 ml of media is suitable for each well. Thus, a dose of BRT-AMS (52.5 μg BRT/1.26 mg AMS) is considered when administrating to the eye at a concentration (1.26 mg BRT-AMS/2 ml media) in the range of BRT-AMS concentrations.

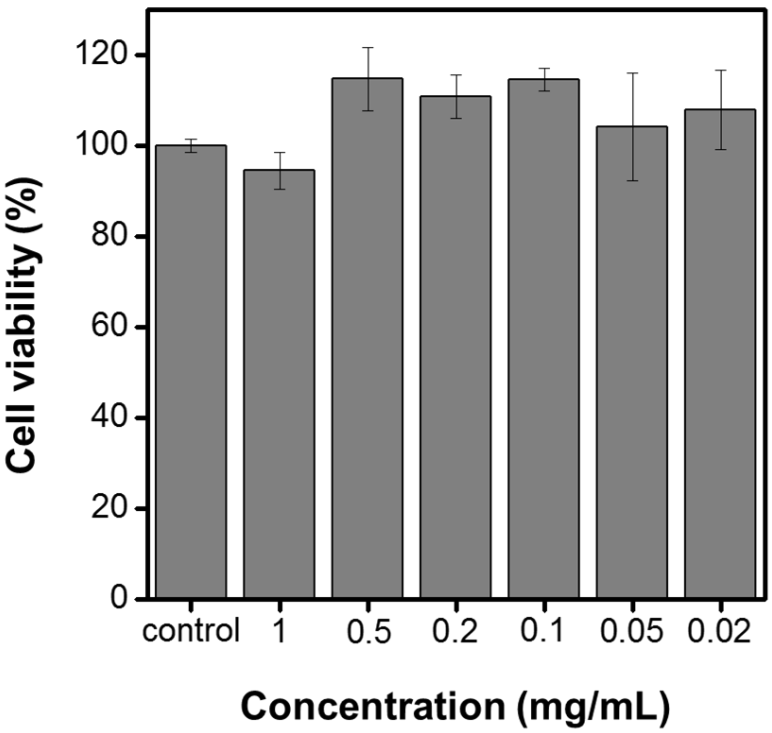

Figure 12. Cell viability assay of BRT-AMS with human corneal epithelial cells (HCECs). Error bars represent standard deviation.

3.5. *In vivo* mucoadhesion study

To examine the mucoadhesive properties in *in vivo*, the percentage of the remaining particles on the precoular surface was measured at the scheduled time point after administrating BRT-AMS particles. Among the initially administrated particles, 65 and 25% remained at 30 min and 4 h, respectively (Figure 13). It was the remarkable result considering that drug bioavailability of the eye drop is less than 5% due to the rapid turnover rate of tear, and that the nanostructured mucoadhesive PLGA/PEG microparticles developed in our previous studies showed less than 4% of particles remained on the eye 2 h after administration (42).

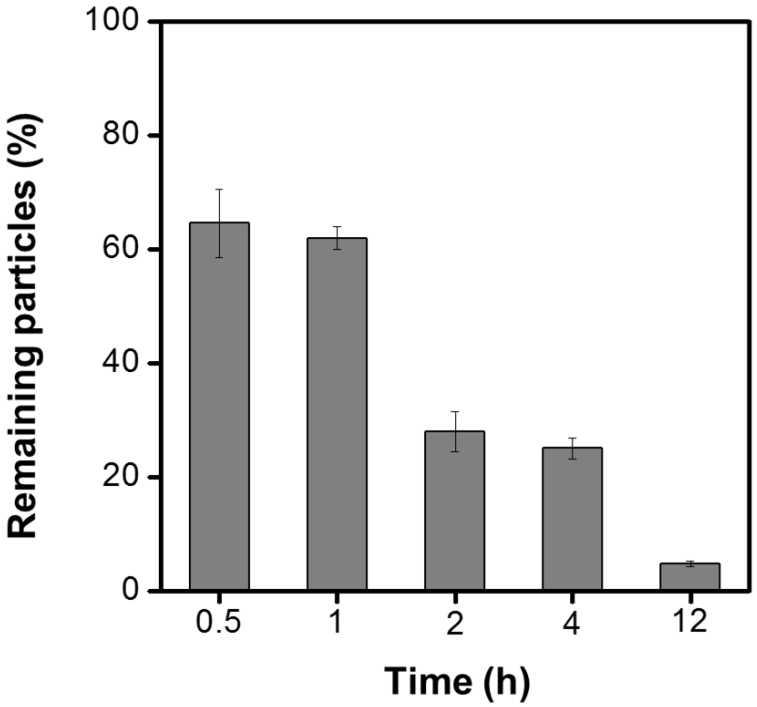

Figure 13. *In vivo* evaluation of preocular retention of BRT-AMS on the rabbit eye. Si weight of particles left on rabbit eye was measured at scheduled intervals after administration. Error bars represent standard deviation.

3.6. *In vivo* study of efficacy and drug bioavailability

The efficacy was evaluated by measuring the decrease in IOP level due to BRT and then comparing that of BRT-AMS with that of Alphagan P. The IOP lowering effect of BRT-AMS was twice as effective as that of Alphagan P considering the activity period (Figure 14). IOP had been reduced by Alphagan P for 6 h, but BRT-AMS reduced for 12 h.

The drug bioavailability of BRT-AMS was improved when comparing the drug concentrations in the aqueous humor (AH) of BRT-AMS and Alphagan P (Figure 15). The drug could be detectable for 8 and 5 h, with BRT-AMS and Alphagan P, respectively. In addition, the area under the curve (AUC) of BRT-AMS was 2.68 μg·h/ml and one of Alphagan P was 1.6 μg·h/ml, respectively. Although the peak drug concentrations (C_{max}) in both of them were not significantly different at the same time (T_{max} = 1 h), the drug concentrations of BRT-AMS were significantly different from those of Alphagan P at 0.25-6 h, except for 1h ($p < 0.05$). Until approximately 40 min, BRT-AMS had lower drug concentrations than Alphagan P due to sustained drug release, but after that this trend was reversed.

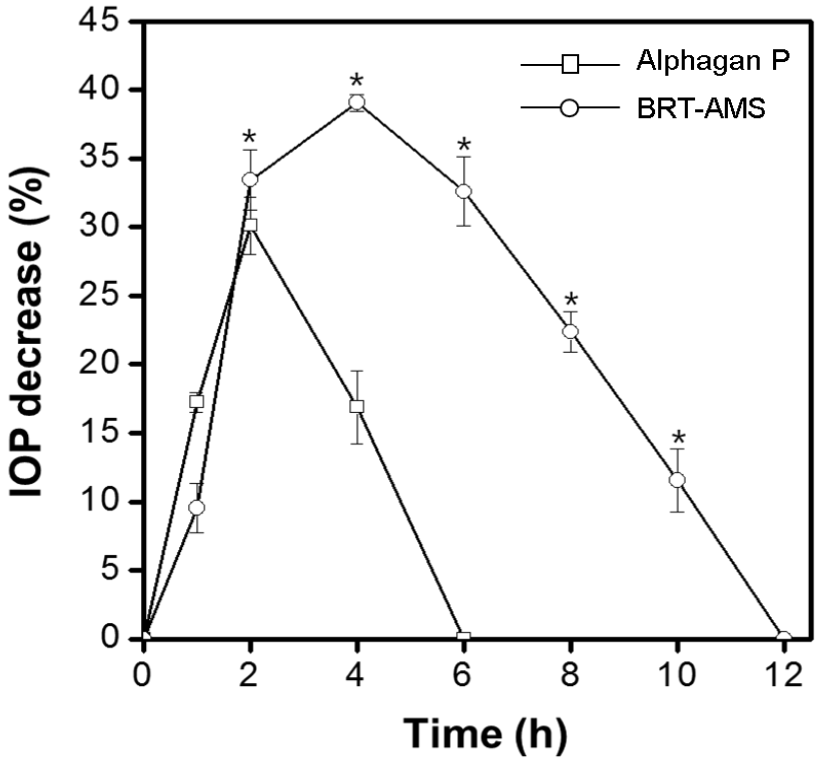

Figure 14. Percent decrease in intraocular pressure (IOP) over time after administration of Alphagan P and BRT-AMS. *BRT-AMS was statistically significantly different from Alphagan P ($p < 0.05$). Error bars represent standard deviation.

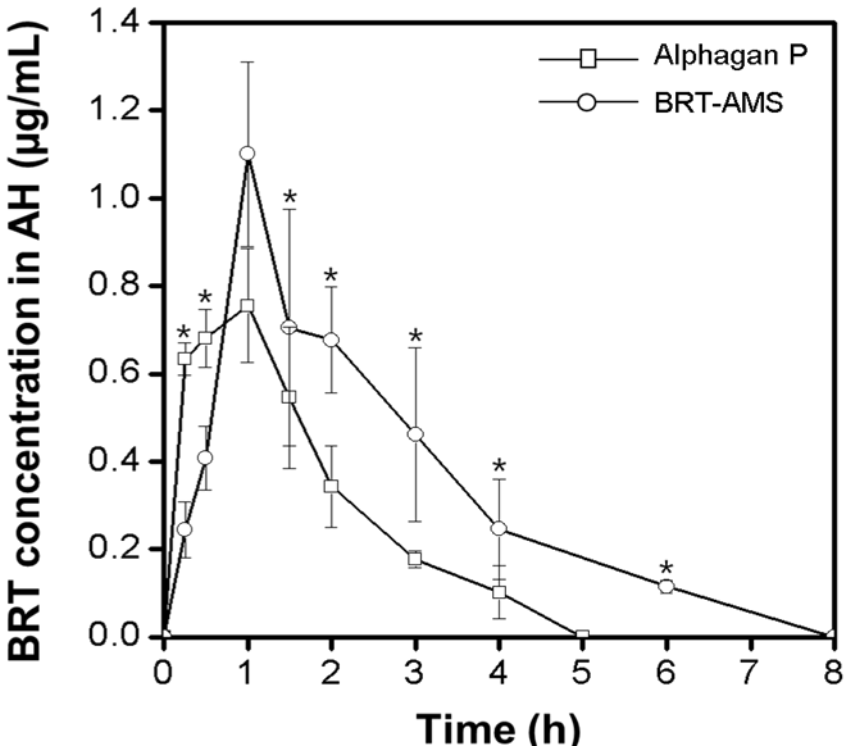

Figure 15. Brimonidine concentrations in the aqueous humor (AH) over time after administration of Alphagan P and BRT-AMS. *BRT-AMS was statistically significantly different from Alphagan P ($p < 0.05$). Error bars represent standard deviation.

Ⅳ. Discussion

Since the discovery of mesoporous materials by Mobil Company (43, 44) and Kuroda *et al.* (45) in the early 1990s to broaden the range of applications for zeolites, they have received considerable attention due to the many advantages (high surface area, versatile surface modification, *etc.*) (46-52). The formation of mesoporous materials is fundamentally based on sol-gel chemistry, but their types are extremely diverse *via* adjusting the interaction between organic species like surfactants and inorganic species like silica oligomers. This means changing the kinds of surfactant (cationic-, non-ionic-, and anionic-) and controlling the pH of the reaction system (53-58). Therefore, many applications for mesoporous silica have been consistently developed in various fields including catalysis, adsorbent materials for separation or molecular sieving, sensing, and carriers for biomedicine (59-66). In particular, research on mesoporous silica as a drug delivery system has increased exponentially since the first report in 2001 due to the outstanding advantages of high drug loading amount, stimuli-responsive drug release profiles, biocompatibility, and easy multifunctionalization (48, 61, 65, 67-73). For effective drug loading and sustained drug release, many approaches have been employed, such as pore size control, surface modification, PEGylation, and so on (67, 73-83).

Among various types of mesoporous silica, AMS, which was first synthesized in 2003, has special characteristics like amine-functionalization in one step and better detergency than cationic surfactant-mediated mesoporous silica. The facile hydrothermal synthesis of AMS particles *via* $S^-X^+I^-$ mechanism is conducted as schematically represented in Scheme 1. Unlike other typical mesoporous silica particles mainly fabricated using a cationic surfactant, AMS was prepared by sodium dodecyl sulfate (SDS) as

an anionic surfactant. Therefore, a CSDA was needed to interact a negatively charged surfactant (S^-) with negatively charged silica species (I^-) under basic conditions (pH > 1.2) considering that the isoelectric point (pI) of silica is around 1.2. Among various CSDA candidates, such as amino silane or quarternary ammonium silane, APTES was used to form highly ordered mesostructures and its positively charged amine groups (X^+) could interact electrostatically with negatively charged surfactant (S^-). This can lead to co-condensing with tetraalkoxysilane of TEOS, resulting in the silica framework formation.

Mucin, the primary component of mucus, has glycoprotein subunits with negative charge at physiological pH since it consists of a protein core and polysaccharide side chains, which mainly terminate in fucose or sialic acid (N-acetylneuraminic acid, pKa=2.6) (13, 15, 84). Thus, the positively charged chitosan has been widely used for mucoadhesive systems as its amino groups can form electrostatic interactions with negatively charged mucin (85-87). Furthermore, a number of studies on the thiolated modification of carriers have shown that they possess mucoadhesion by disulfide bonds with cysteine-rich mucin domains (88-91). In this work, the mucoadhesive property of amine-functionalized AMS was studied with respect to making new bonds between AMS and mucin such as amide groups and hydrogen bonds, rather than the electrostatic interaction between positively charged amine groups and negatively charged mucus layer of the eye. This means that mucoadhesion of AMS is derived from newly formed amide groups through a condensation reaction between the amine group of AMS and carbonyl group of mucin. Thereby, a significant amount of mucin was adsorbed by AMS or BRT-AMS, which was revealed in the zeta potential shift of BRT-AMS toward mucin after mixing BRT-AMS and

mucin solution. In addition, BRT-AMS adsorbed more mucin than AMS as shown in Figure 9, because BRT has many unshared electrons on nitrogen and bromine. Therefore, BRT-AMS had stronger anionic charge than AMS, which was supported by the zeta potential values in DI water, -32.66 mV of BRT-AMS and -14.60 mV of AMS (data was not shown). A more apparent electron distortion could make BRT-AMS have more hydrogen bonds with mucin (14, 92-94).

Brimonidine (BRT) can be effectively encapsulated into AMS particles as attributed to the positively charged amine groups on AMS and large surface area of AMS. In other words, the negatively charged BRT is encapsulated into amine-functionalized AMS *via* electrostatic attraction as well as physical adsorption due to the large AMS surface area. Thus, the loading amount of BRT (41.73 μg/mg) was sufficient for BRT-AMS, so that a single dose of BRT, 52.5 μg, can be delivered with 1.26 mg of BRT-AMS particles. The loaded BRT was slowly released for 8 h, although the high-rate release of BRT existed at the beginning of the *in vitro* drug release profile test due to the hydrophilic drug, BRT (Figure 8).

Brimonidine [5-boromo-6-(2-imidazolidinylideneamino) quinoxaline L] has been used as an ocular hypotensive agent by decreasing aqueous humor production and increasing uveoscleral outflow (38, 95, 96). Thus, I evaluated the improved efficacy of BRT-AMS by measuring the decreased profiles in IOP and confirmed that the duration of drug action of BRT-AMS was twice as long as that of Alphagan P, the commercialized eye drop (Figure 14). This could be explained by the mucoadhesive property that prevented BRT-AMS particles from being washed away and the remained particles on the mucus layer that slowly released BRT (12, 29, 97) due to the mesopores inside AMS particles. For the *in vivo* drug bioavailability test, the

mucoadhesive property of BRT-AMS caused the drug bioavailability to be enhanced (Figure 15). Although its drug concentration in aqueous humor was lower than that of Alphagan P for 1h after administration, it was a reasonable result considering that BRT-AMS sustained the drug release (90, 98, 99).

Ⅴ. Conclusion

A new ocular drug delivery system for glaucoma treatment by preparing BRT-AMS particles is presented in this paper. The spherical AMS particles can be successfully obtained with optimal size for administration to the eye. The amine-functionalized AMS particles form a new bond with the carboxyl groups of mucin, which work with a mechanism of mucoadhesion for AMS particles to better remain in the preocular surface. Furthermore, AMS with large surface area efficiently encapsulated the negatively charged BRT and released it in a controlled manner, while BRT-AMS was biocompatible in the cytotoxicity test of HCECs. Thereby, BRT-AMS exhibited improved efficacy and drug bioavailability. In conclusion, mucoadhesive AMS is a promising carrier as a glaucoma drug delivery system.

Ⅵ. References

1. Quigley HA, Broman AT. The number of people with glaucoma worldwide in 2010 and 2020. Br J Ophthalmol. 2006;90(3):262-7.
2. Kingman S. Glaucoma is second leading cause of blindness globally. B World Health Organ. 2004;82(11):887-8.
3. Kass MA, Heuer DK, Higginbotham EJ, Johnson CA, Keltner JL, Miller JP, et al. The Ocular Hypertension Treatment Study - A randomized trial determines that topical ocular hypotensive medication delays or prevents the onset of primary open-angle glaucoma. Arch Ophthalmol-Chic. 2002;120(6):701-13.
4. Patel SC, Spaeth GL. Compliance in Patients Prescribed Eyedrops for Glaucoma. Ophthalmic Surg Las. 1995;26(3):233-6.
5. Urtti A. Challenges and obstacles of ocular pharmacokinetics and drug delivery. Adv Drug Deliver Rev. 2006;58(11):1131-5.
6. Gaudana R, Jwala J, Boddu SH, Mitra AK. Recent perspectives in ocular drug delivery. Pharm Res. 2009;26(5):1197-216.
7. Zimmer A, Kreuter J. Microspheres and Nanoparticles Used in Ocular Delivery Systems. Adv Drug Deliver Rev. 1995;16(1):61-73.
8. Le Bourlais C, Acar L, Zia H, Sado PA, Needham T, Leverge R. Ophthalmic drug delivery systems - Recent advances. Progress in Retinal and Eye Research. 1998;17(1):33-58.
9. Sahoo SK, Diinawaz F, Krishnakumar S. Nanotechnology in ocular drug delivery. Drug Discovery Today. 2008;13(3-4):144-51.
10. Peng CC, Burke MT, Carbia BE, Plummer C, Chauhan A. Extended drug delivery by contact lenses for glaucoma therapy. Journal of Controlled Release. 2012;162(1):152-8.
11. Sultana Y, Jain R, Aqil M, Ali A. Ocular drug delivery systems: An overview. Curr Drug Deliv. 2006;3(2):207-17.

12. Kapanigowda UG, Nagaraja SH, Ramaiah B, Boggarapu PR. Improved intraocular bioavailability of ganciclovir by mucoadhesive polymer based ocular microspheres: development and simulation process in Wistar rats. Daru. 2015;23.
13. Andrews GP, Laverty TP, Jones DS. Mucoadhesive polymeric platforms for controlled drug delivery. European Journal of Pharmaceutics and Biopharmaceutics. 2009;71(3):505-18.
14. Buri NAPaPA. SURFACE, INTERFACIAL AND MOLECULAR ASPECTS OF POLYMER BIOADHESION ON SOFT TISSUES. Journal of Controlled Release. 1985;2.
15. Ludwig A. The use of mucoadhesive polymers in ocular drug delivery. Adv Drug Deliver Rev. 2005;57(11):1595-639.
16. Chong ASM, Zhao XS. Functionalization of SBA-15 with APTES and characterization of functionalized materials. J Phys Chem B. 2003;107(46):12650-7.
17. Salmio H, Bruhwiler D. Distribution of amino groups on a mesoporous silica surface after submonolayer deposition of aminopropylsilanes from an anhydrous liquid phase. J Phys Chem C. 2007;111(2):923-9.
18. Aguado J, Arsuaga JM, Arencibia A, Lindo M, Gascon V. Aqueous heavy metals removal by adsorption on amine-functionalized mesoporous silica. J Hazard Mater. 2009;163(1):213-21.
19. Benhamou A, Baudu M, Derriche Z, Basly JP. Aqueous heavy metals removal on amine-functionalized Si-MCM-41 and Si-MCM-48. J Hazard Mater. 2009;171(1-3):1001-8.
20. Nomura A, Jones CW. Amine-Functionalized Porous Silicas as Adsorbents for Aldehyde Abatement. Acs Appl Mater Inter. 2013;5(12):5569-77.
21. Moschetta EG, Sakwa-Novak MA, Greenfield JL, Jones CW. Post-Grafting Amination of Alkyl Halide-Functionalized Silica for Applications in

Catalysis, Adsorption, and15N NMR Spectroscopy. Langmuir. 2015;31(7):2218-27.
22. Cantor LB. Brimonidine in the treatment of glaucoma and ocular hypertension. Ther Clin Risk Manag. 2006;2(4):337-46.
23. Yokoi T, Yoshitake H, Tatsumi T. Synthesis of anionic-surfactant-templated mesoporous silica using organoalkoxysilane-containing amino groups. Chemistry of Materials. 2003;15(24):4536-8.
24. In vitro evaluation of the mucoadhesive properties of chitosan microspheres. International Journal of Pharmaceutics. 1998.
25. Lee DW, Shirley SA, Lockey RF, Mohapatra SS. Thiolated chitosan nanoparticles enhance anti-inflammatory effects of intranasally delivered theophylline. Respir Res. 2006;7:112.
26. Chitosan Nanoparticles as New Ocular Drug Delivery Systems: in Vitro Stability, in Vivo Fate, and Cellular Toxicity. Pharmaceutical Research. 2004.
27. Sriamornsak P, Wattanakorn N, Takeuchi H. Study on the mucoadhesion mechanism of pectin by atomic force microscopy and mucin-particle method. Carbohydrate Polymers. 2010;79(1):54-9.
28. Kim T, Lee H, Kim Y, Nam JM, Lee M. Protein-coated nanofibers for promotion of T cell activity. Chem Commun (Camb). 2013;49(38):3949-51.
29. Park CG, Kim YK, Kim MJ, Park M, Kim MH, Lee SH, et al. Mucoadhesive microparticles with a nanostructured surface for enhanced bioavailability of glaucoma drug. J Control Release. 2015;220(Pt A):180-8.
30. Park CG, Kim MJ, Park M, Choi SY, Lee SH, Lee JE, et al. Nanostructured mucoadhesive microparticles for enhanced preocular retention. Acta Biomater. 2014;10(1):77-86.
31. Dong JQ, Babusis DM, Welty DF, Acheampong AA, Tang-Liu D, Whitcup SM. Effects of the preservative Puriteo((R)) on the bioavailability

of brimonidine in the aqueous humor of rabbits. Journal of Ocular Pharmacology and Therapeutics. 2004;20(4):285-92.

32. Bin Choy Y, Park JH, Prausnitz MR. Mucoadhesive microparticles engineered for ophthalmic drug delivery. J Phys Chem Solids. 2008;69(5-6):1533-6.

33. Ramimoghadam D, Bin Hussein MZ, Taufiq-Yap YH. The Effect of Sodium Dodecyl Sulfate (SDS) and Cetyltrimethylammonium Bromide (CTAB) on the Properties of ZnO Synthesized by Hydrothermal Method. International Journal of Molecular Sciences. 2012;13(10):13275-93.

34. Suteewong T, Sai H, Bradbury M, Estroff LA, Gruner SM, Wiesner U. Synthesis and Formation Mechanism of Aminated Mesoporous Silica Nanoparticles. Chemistry of Materials. 2012;24(20):3895-905.

35. Sing KSW, Everett DH, Haul RAW, Moscou L, Pierotti RA, Rouquerol J, et al. Reporting Physisorption Data for Gas Solid Systems with Special Reference to the Determination of Surface-Area and Porosity (Recommendations 1984). Pure Appl Chem. 1985;57(4):603-19.

36. Kim S-N, Son W-J, Choi J-S, Ahn W-S. CO2 adsorption using amine-functionalized mesoporous silica prepared via anionic surfactant-mediated synthesis. Microporous and Mesoporous Materials. 2008;115(3):497-503.

37. Jaroniec MKaM. Gas Adsorption Characterization of Ordered Organic−Inorganic Nanocomposite Materials. Chem Mater. 2001;13.

38. Prakash Bhagav PD, Saurabh Pandey, Sajeev Chandran. Development and Validation of Stability Indicating UV Spectrophotometric Method for the Estimation of Brimonidine Tartrate in Pure Form, Formulations and Preformulation Studies. Der Pharmacia Lettre. 2010;2(3):106-22.

39. Elizabeth Fonseca dos Reis, Fábia S. Campos, Andrey Pereira Lagea, Romulo Cerqueira Leite, Luiz Guilherme Heneine, Wander Luiz Vasconcelos, et al. Synthesis and characterization of poly (vinyl alcohol)

hydrogels and hybrids for rMPB70 protein adsorption. Materials Research. 2006;9(2).

40. Jadhav SA, Bongiovanni R, Marchisio DL, Fontana D, Egger C. Surface modification of iron oxide (Fe2O3) pigment particles with amino-functional polysiloxane for improved dispersion stability and hydrophobicity. Pigm Resin Technol. 2014;43(4):219-27.

41. Braz WR, Rocha NL, de Faria EH, Silva MLAE, Ciuffi KJ, Tavares DC, et al. Incorporation of anti-inflammatory agent into mesoporous silica. Nanotechnology. 2016;27(38).

42. Park CG, Kim MJ, Park M, Choi SY, Lee SH, Lee JE, et al. Nanostructured mucoadhesive microparticles for enhanced preocular retention. Acta Biomaterialia. 2014;10(1):77-86.

43. Kresge CT, Leonowicz ME, Roth WJ, Vartuli JC, Beck JS. Ordered Mesoporous Molecular-Sieves Synthesized by a Liquid-Crystal Template Mechanism. Nature. 1992;359(6397):710-2.

44. Beck JS, Vartuli JC, Roth WJ, Leonowicz ME, Kresge CT, Schmitt KD, et al. A New Family of Mesoporous Molecular-Sieves Prepared with Liquid-Crystal Templates. J Am Chem Soc. 1992;114(27):10834-43.

45. Inagaki S, Fukushima Y, Kuroda K. Synthesis of Highly Ordered Mesoporous Materials from a Layered Polysilicate. J Chem Soc Chem Comm. 1993(8):680-2.

46. Slowing, II, Vivero-Escoto JL, Wu CW, Lin VS. Mesoporous silica nanoparticles as controlled release drug delivery and gene transfection carriers. Adv Drug Deliv Rev. 2008;60(11):1278-88.

47. MSN_biofunctionality and biocompatibility. ACCOUNTS OF CHEMICAL RESEARCH 2012.

48. Tang F, Li L, Chen D. Mesoporous silica nanoparticles: synthesis, biocompatibility and drug delivery. Adv Mater. 2012;24(12):1504-34.

49. Argyo C, Weiss V, Bräuchle C, Bein T. Multifunctional Mesoporous Silica Nanoparticles as a Universal Platform for Drug Delivery. Chemistry of Materials. 2014;26(1):435-51.
50. Gibson LT. Mesosilica materials and organic pollutant adsorption: part A removal from air. Chem Soc Rev. 2014;43(15):5163-72.
51. Palanikumar L, Choi ES, Cheon JY, Joo SH, Ryu J-H. Noncovalent Polymer-Gatekeeper in Mesoporous Silica Nanoparticles as a Targeted Drug Delivery Platform. Advanced Functional Materials. 2015;25(6):957-65.
52. Wang H, Rong X, Han L, Tang M, Yu M, Zhang J, et al. Controlled synthesis of hexagonal mesostructure silica and macroporous ordered siliceous foams for VOCs adsorption. RSC Adv. 2015;5(8):5695-703.
53. Lin HP, Mou CY. Structural and morphological control of cationic surfactant-templated mesoporous silica. Accounts of Chemical Research. 2002;35(11):927-35.
54. Chao MC, Lin HP, Mou CY, Cheng BW, Cheng CF. Synthesis of nano-sized mesoporous silicas with metal incorporation. Catal Today. 2004;97(1):81-7.
55. Jorge M, Gomes JRB, Cordeiro MNDS, Seaton NA. Molecular Dynamics Simulation of the Early Stages of the Synthesis of Periodic Mesoporous Silica. J Phys Chem B. 2009;113(3):708-18.
56. Michaux F, Baccile N, Imperor-Clerc M, Malfatti L, Folliet N, Gervais C, et al. In Situ Time-Resolved SAXS Study of the Formation of Mesostructured Organically Modified Silica through Modeling of Micelles Evolution during Surfactant-Templated Self-Assembly. Langmuir. 2012;28(50):17477-93.
57. Blin JL, Imperor-Clerc M. Mechanism of self-assembly in the synthesis of silica mesoporous materials: in situ studies by X-ray and neutron scattering. Chemical Society Reviews. 2013;42(9):4071-82.
58. Wu SH, Mou CY, Lin HP. Synthesis of mesoporous silica nanoparticles. Chem Soc Rev. 2013;42(9):3862-75.

59. Corma A. From microporous to mesoporous molecular sieve materials and their use in catalysis. Chem Rev. 1997;97(6):2373-419.
60. Unger KK, Kumar D, Grun M, Buchel G, Ludtke S, Adam T, et al. Synthesis of spherical porous silicas in the micron and submicron size range: challenges and opportunities for miniaturized high-resolution chromatographic and electrokinetic separations. J Chromatogr A. 2000;892(1-2):47-55.
61. Vallet-Regi M, Ramila A, del Real RP, Perez-Pariente J. A new property of MCM-41: Drug delivery system. Chemistry of Materials. 2001;13(2):308-11.
62. Raja R, Thomas JM. Catalyst design strategies for controlling reactions in microporous and mesoporous molecular-sieves. J Mol Catal a-Chem. 2002;181(1-2):3-14.
63. Zhou L, Liu XW, Li JW, Wang N, Wang Z, Zhou YP. Synthesis of ordered mesoporous carbon molecular sieve and its adsorption capacity for H-2, N-2, O-2, CH4 and CO2. Chemical Physics Letters. 2005;413(1-3):6-9.
64. Melde BJ, Johnson BJ, Charles PT. Mesoporous silicate materials in sensing. Sensors-Basel. 2008;8(8):5202-28.
65. Slowing II, Vivero-Escoto JL, Wu CW, Lin VSY. Mesoporous silica nanoparticles as controlled release drug delivery and gene transfection carriers. Adv Drug Deliver Rev. 2008;60(11):1278-88.
66. Halder P, Maurya M, Jain SK, Singh JK. Understanding adsorption of CO2, N2, CH4 and their mixtures in functionalized carbon nanopipe arrays. Phys Chem Chem Phys. 2016;18(20):14007-16.
67. Vallet-Regi M, Balas F, Arcos D. Mesoporous materials for drug delivery. Angew Chem Int Ed Engl. 2007;46(40):7548-58.
68. Manzano M, Aina V, Arean CO, Balas F, Cauda V, Colilla M, et al. Studies on MCM-41 mesoporous silica for drug delivery: Effect of particle morphology and amine functionalization. Chem Eng J. 2008;137(1):30-7.

69. Cauda V, Argyo C, Schlossbauer A, Bein T. Controlling the delivery kinetics from colloidal mesoporous silica nanoparticles with pH-sensitive gates. Journal of Materials Chemistry. 2010;20(21):4305-11.
70. Szegedi A, Popova M, Goshev I, Mihaly J. Effect of amine functionalization of spherical MCM-41 and SBA-15 on controlled drug release. J Solid State Chem. 2011;184(5):1201-7.
71. Ukmar T, Maver U, Planinsek O, Kaucic V, Gaberscek M, Godec A. Understanding controlled drug release from mesoporous silicates: Theory and experiment. Journal of Controlled Release. 2011;155(3):409-17.
72. Szegedi A, Popova M, Goshev I, Klebert S, Mihaly J. Controlled drug release on amine functionalized spherical MCM-41. J Solid State Chem. 2012;194:257-63.
73. Argyo C, Weiss V, Brauchle C, Bein T. Multifunctional Mesoporous Silica Nanoparticles as a Universal Platform for Drug Delivery. Chemistry of Materials. 2014;26(1):435-51.
74. Liberman A, Mendez N, Trogler WC, Kummel AC. Synthesis and surface functionalization of silica nanoparticles for nanomedicine. Surf Sci Rep. 2014;69(2-3):132-58.
75. Yanes RE, Tamanoi F. Development of mesoporous silica nanomaterials as a vehicle for anticancer drug delivery. Ther Deliv. 2012;3(3):389-404.
76. Siafaka PI, Okur NU, Karavas E, Bikiaris DN. Surface Modified Multifunctional and Stimuli Responsive Nanoparticles for Drug Targeting: Current Status and Uses. International Journal of Molecular Sciences. 2016;17(9).
77. Baeza A, Colilla M, Vallet-Regi M. Advances in mesoporous silica nanoparticles for targeted stimuli-responsive drug delivery. Expert Opin Drug Del. 2015;12(2):319-37.

78. Gulzar A, Gai SL, Yang PP, Li CX, Ansari MB, Lin J. Stimuli responsive drug delivery application of polymer and silica in biomedicine. J Mater Chem B. 2015;3(44):8599-622.
79. Song YH, Li YH, Xu Q, Liu Z. Mesoporous silica nanoparticles for stimuli-responsive controlled drug delivery: advances, challenges, and outlook. Int J Nanomed. 2017;12:87-110.
80. Yang PP, Gai SL, Lin J. Functionalized mesoporous silica materials for controlled drug delivery. Chemical Society Reviews. 2012;41(9):3679-98.
81. Zhang Q, Liu F, Nguyen KT, Ma X, Wang XJ, Xing BG, et al. Multifunctional Mesoporous Silica Nanoparticles for Cancer-Targeted and Controlled Drug Delivery. Advanced Functional Materials. 2012;22(24):5144-56.
82. Pang J, Luan Y, Yang X, Jiang Y, Zhao L, Zong Y, et al. Functionalized Mesoporous Silica Particles for Application in Drug Delivery System. Mini-Rev Med Chem. 2012;12(8):775-88.
83. McCarthy CA, Ahern RJ, Dontireddy R, Ryan KB, Crean AM. Mesoporous silica formulation strategies for drug dissolution enhancement: a review. Expert Opin Drug Del. 2016;13(1):93-108.
84. Serra L, Domenech J, Peppas NA. Engineering design and molecular dynamics of mucoadhesive drug delivery systems as targeting agents. European Journal of Pharmaceutics and Biopharmaceutics. 2009;71(3):519-28.
85. He P, Davis SS, Illum L. In vitro evaluation of the mucoadhesive properties of chitosan microspheres. International Journal of Pharmaceutics. 1998;166(1):75-88.
86. Agnihotri SA, Mallikarjuna NN, Aminabhavi TM. Recent advances on chitosan-based micro- and nanoparticles in drug delivery. Journal of Controlled Release. 2004;100(1):5-28.
87. Smart JD. The basics and underlying mechanisms of mucoadhesion. Adv Drug Deliver Rev. 2005;57(11):1556-68.

88. Davidovich-Pinhas M, Harari O, Bianco-Peled H. Evaluating the mucoadhesive properties of drug delivery systems based on hydrated thiolated alginate. Journal of Controlled Release. 2009;136(1):38-44.
89. Shen J, Wang Y, Ping QN, Xiao YY, Huang X. Mucoadhesive effect of thiolated PEG stearate and its modified NLC for ocular drug delivery. Journal of Controlled Release. 2009;137(3-4):217-23.
90. Shen J, Deng YP, Jin XF, Ping QN, Su ZG, Li LJ. Thiolated nanostructured lipid carriers as a potential ocular drug delivery system for cyclosporine A: Improving in vivo ocular distribution. International Journal of Pharmaceutics. 2010;402(1-2):248-53.
91. Zhang Q, Neoh KG, Xu LQ, Lu SJ, Kang ET, Mahendran R, et al. Functionalized Mesoporous Silica Nanoparticles with Mucoadhesive and Sustained Drug Release Properties for Potential Bladder Cancer Therapy. Langmuir. 2014;30(21):6151-61.
92. Peppas NA, Thomas JB, McGinty J. Molecular Aspects of Mucoadhesive Carrier Development for Drug Delivery and Improved Absorption. J Biomat Sci-Polym E. 2009;20(1):1-20.
93. Boddupalli BM, Mohammed ZN, Nath RA, Banji D. Mucoadhesive drug delivery system: An overview. J Adv Pharm Technol Res. 2010;1(4):381-7.
94. Shinkar DM, Dhake AS, Setty CM. Drug delivery from the oral cavity: a focus on mucoadhesive buccal drug delivery systems. PDA J Pharm Sci Technol. 2012;66(5):466-500.
95. Munk SA, Harcourt D, Arasasingham P, Gluchowski C, Wong H, Burke J, et al. Analogs of Uk-14,304 - Structural Features Responsible for Alpha(2) Adrenoceptor Activity. Bioorganic & Medicinal Chemistry Letters. 1995;5(15):1745-50.
96. Toris CB, Camras CB, Yablonski ME. Acute versus chronic effects of brimonidine on aqueous humor dynamics in ocular hypertensive patients. American Journal of Ophthalmology. 1999;128(1):8-14.

97. Tayel SA, El-Nabarawi MA, Tadros MI, Abd-Elsalam WH. Promising ion-sensitive in situ ocular nanoemulsion gels of terbinafine hydrochloride: Design, in vitro characterization and in vivo estimation of the ocular irritation and drug pharmacokinetics in the aqueous humor of rabbits. International Journal of Pharmaceutics. 2013;443(1-2):293-305.
98. Clark TS, Clark DD, Hoyt RF, Jr. Pharmacokinetic comparison of sustained-release and standard buprenorphine in mice. J Am Assoc Lab Anim Sci. 2014;53(4):387-91.
99. Jogala S, Rachamalla SS, Aukunuru J. Development of subcutaneous sustained release nanoparticles encapsulating low molecular weight heparin. J Adv Pharm Technol. 2015;6(2):58-64.

국문 초록

음이온 계면활성제 매개 메조포러스 실리카 입자를 이용한 녹내장 약물의 국소 점안 전달

본 연구에서는 녹내장 약물 전달체를 개발하였고, 효과적인 전달체가 되도록 전안부에서의 약물 거주시간을 증가시키기 위해 점막 부착성을 지니는 것을 목표로 하였다. 뿐만 아니라, 눈에 투여하는 입자량을 줄이고자 전달체가 높은 약물담지량을 갖도록 하였고, 담지된 약물은 전달체에서 서서히 방출되도록 하였다. 녹내장 약물은 안압을 낮추는 기능을 갖는 브리모니딘(BRT)을 사용했고, 전달체로는 별도의 후 처리 과정 없이 $S^{-}X^{+}I^{-}$ 메커니즘을 통해 입자 합성 과정에서 입자 표면에 아민기가 결합되는 음이온 계면활성제 매개 메조포러스 실리카(AMS)를 사용하였다. 제작된 약 1 μm 크기의 AMS 구형 입자는 다른 메조포러스 실리카 물질과 같이 입자 내부에 무수히 많은 세공을 지녀 넓은 비표면적(544.1 m^2/g)을 보였고, 많은 양의 BRT 을 탑재(41.73 μg/mg)하였다. 또한 시험관 내 약물 방출 실험에서 확인한 결과, 입자의 세공을 통하여 입자 내 담지된 BRT 이 8 시간

동안 지속적으로 방출되었다. 본 연구의 가장 핵심적인 내용인 BRT 을 담지한 AMS (BRT-AMS) 입자의 점막 부착 특성을 평가하는 것은 크게 세 가지 방법으로 진행되었다. 첫 번째로 점막의 구성 성분인 뮤신 1 mg 중 약 0.6 mg 이 BRT-AMS 입자 2 mg 에 흡착 되었음을 확인하였고, 두 번째로 BRT-AMS 의 제타 전위 값이 뮤신과 흡착한 이후 뮤신의 제타 전위 값으로 이동하였음을 관찰하였다. 이러한 BRT-AMS 의 점막 부착성은 FTIR 을 통해 AMS 의 아민기와 뮤신의 카르복실기 사이에 새롭게 형성된 아마이드 결합으로 인한 것임을 입증하였다. 세 번째 평가방법으로 토끼의 눈에 BRT-AMS 입자를 투여한 후 시간이 지남에 따라 전안부에 남아있는 입자의 양을 측정해보았다. 이 때, 입자를 투여한 후 4 시간이 지나더라도 처음 투여한 입자량의 25%가 토끼 눈에 남아있음을 확인하였다. 또한 인간 각막 상피 세포를 이용한 세포 독성 시험에서 BRT-AMS 의 생체적합성을 확인하였다. 이처럼 점막 부착성과 생체적합성을 갖는 BRT-AMS 는 전안부에 오래 거주하여 녹내장의 상용화 약물인 알파간피(Alphagan P)보다 두 배 더 긴 12 시간 동안 안압 하강 효과를 나타냈으며, 토끼 눈의 방수 내 BRT 농도 역시 알파간 피보다 높음을 보임으로써 약물생체이용도가 증가됨을 확인하였다. 이로써 본 연구에서는 BRT-AMS 를 제작하여 제형의 높은 약물 담지량 및 약물 서방출성, 점막 부착성으로 인해 향상된 약물 효과와 약물생체이용도를 확인하였다. 이를 통해 AMS 가 녹내장 약물 전달체로서 적합함을 증명하였고, 체내 점막으로 이루어진 기관으로의 약물 전달체로 이용 가능함을 발견하였다.

주 요 어: 녹내장, 메조포러스 실리카, 점막 부착성, 안구 약물 전달, 브리모니딘

학 번: 2015-22884